Retention and remobilization of colloids during steady-state and transient two-phase flow

Qiulan Zhang,[1] S. M. Hassanizadeh,[1,2] N. K. Karadimitriou,[1] A. Raoof,[1] Bing Liu,[3] P. J. Kleingeld,[1] and A. Imhof[3]

Received 29 June 2013; revised 4 November 2013; accepted 6 November 2013; published 6 December 2013.

[1] In this work, we study colloid transport through a porous medium under steady-state and transient two-phase flow conditions. The porous medium was a PDMS micromodel and the immiscible fluids were water and fluorinert-FC43. Given that the micromodel was hydrophobic, fluorinert was the wetting phase, and water was the nonwetting phase. We used hydrophilic fluorescent microspheres (dispersed in water) with mean diameter of 300 nm. We directly observed colloid movement and fluids distribution within pores of the micromodel using a confocal laser scanning microscope. We also obtained concentration breakthrough curves by measuring the fluorescence intensity in the outlet of the micromodel. The breakthrough curves showed that, under steady-state flow at different water saturations, more colloids were retained at lower saturations. Our visualization results suggested that the enhanced attachment was due to the retention of colloids onto fluorinert-water interfaces (FWIs) and fluorinert-water-solid contact lines (FWSCs). At the end of a steady-state two-phase flow experiment, we changed the micromodel saturation by injecting either water (drainage) or fluorinert (imbibition). We found remobilization of colloids during imbibition events, but no remobilization was observed during drainage. Visualization showed that colloids deposited on solid-water interfaces (SWIs) were dislodged by moving FWSCs during imbibition. We simulated breakthrough curves by modeling colloids interactions with SWIs and FWIs separately. Remobilization of colloids attached to SWI was modeled as a first-order kinetic process and the rate coefficient was assumed proportional to temporal rate of change of saturation. Colloids attachment to and detachment from FWIs were modeled as an equilibrium process. Generally, good agreements between experimental results and simulation were obtained. This is the first study of colloid transport in two-phase flow, where pore-scale visualization, breakthrough concentration measurement, and modeling of results are combined.

Citation: Zhang, Q., S. M. Hassanizadeh, N. K. Karadimitriou, A. Raoof, B. Liu, P. J. Kleingeld, and A. Imhof (2013), Retention and remobilization of colloids during steady-state and transient two-phase flow, *Water Resour. Res.*, *49*, 8005–8016, doi:10.1002/2013WR014345.

1. Introduction

[2] Over the past few decades, considerable research has been done to understand the behavior of colloidal particles and viruses in partially saturated porous media, through laboratory works, field studies, and numerical simulations. An important aspect of colloid behavior is the remobilization of attached colloids. Recently, colloids remobilization has drawn significant attention due to its potential for enhancing contaminant transport through the vadose zone to the groundwater [*Saiers et al*., 2003; *Zhuang et al*., 2009]. Remobilization of colloids has been found to be sensitive to the following factors: properties of colloids and soils [*Bradford and Kim*, 2012], solution ionic strength and pH [*Torkzaban et al*., 2006a; *Zevi et al*., 2009; *Zhuang et al*., 2010; *Sadeghi et al*., 2011], and flow patterns [*Saiers and Lenhart*, 2003; *Torkzaban et al*., 2006a, 2006b; *Shang et al*., 2008; *Zhuang et al*., 2007, 2009; *Cheng and Saiers*, 2009].

[3] In particular, it was observed that temporal changes in flow conditions can cause a significant increase of the rate of colloid detachment. For example, *Saiers and Lenhart* [2003] observed in column experiments that increase in water flow rates and water saturation led to enhanced colloid release, compared to steady-state flow conditions. Similarly, *Shang et al*. [2008] reported remobilization of colloids due to a step increase in water saturation and flow rates. Not only imbibition, but also drainage is found to cause colloids remobilization, as observed by *Zhuang et al*.

Additional supporting information may be found in the online version of this article.

[1]Earth Sciences Department, Utrecht University, Utrecht, Netherlands.
[2]Soil and Groundwater Systems, Deltares, Netherlands.
[3]Soft Condensed Matter, Debye Institute, Utrecht University, Utrecht, Netherlands.

Corresponding author: S. M. Hassanizadeh, Earth Sciences Department, Utrecht University, Budapestlaan 4, NL-3584 CD Utrecht, Netherlands. (S.M.Hassanizadeh@uu.nl)

0043-1397/13/10.1002/2013WR014345

[2007] and *Cheng and Saiers* [2009]. Transients in chemical conditions can also cause colloids remobilization. *Flury et al*. [2003] reported that colloids can be mobilized when low ionic strength pore water displaces high ionic strength pore water. *Bradford et al*. [2012] also found that decrease in ionic strength can result in colloid remobilization. Virus remobilization was observed by *Sadeghi et al*. [2013] when reducing the calcium concentration of the inflow solution, keeping the ionic strength constant.

[4] Colloids transport processes in unsaturated media are complex. Generally, enhanced colloid attachment has been observed at lower saturations. Interestingly, different authors have given different reasons for this enhanced attachment. In some studies, increased colloids retention at lower saturation was mainly attributed to irreversible colloids attachment to air-water interfaces (AWIs) [e.g., *Wan and Wilson*, 1994a, 1994b; *Wan and Tokunaga*, 2002; *Sirivithayapakorn and Keller*, 2003; *Keller and Sirivithayapakorn*, 2004; *Torkzaban et al*., 2006a]. Some other researches, however, have assumed colloid attachment to the AWI to be a reversible process in their numerical modeling [*Torkzaban et al*., 2006b]. Some experimental studies have questioned the significance of colloid attachment to AWI. For example, *Chen and Flury* [2005] suspended an air bubble in a micromodel; they did not observe any colloid attachment to AWI. Another group of researchers, e.g., *Crist et al*. [2004, 2005] and *Zevi et al*. [2005, 2006, 2009], found that air-water-solid (AWS) contact lines are the primary locations for enhanced colloids retention. *Lazouskaya and Jin* [2008] suggested that in a dynamic system, if colloid retention at AWI does not occur in the primary minimum, then colloid retention at AWS becomes dominant. In addition to attachment to SWI, AWI, and AWS; film straining has been reported as another important mechanism for colloids retention under unsaturated conditions [*Wan and Tokunaga*, 1997; *Veerapaneni et al*., 2000]. Apparently, our knowledge of mechanisms of colloids transport in unsaturated porous media is still limited.

[5] Recently, to better understand the above mechanisms, studies involving direct observations of colloid transport in unsaturated porous media have been conducted. Some experiments were performed in a capillary channel with moving air-water interfaces [*Sharma et al*., 2008; *Aramrak et al*., 2011]. Others were performed in a micromodel or in soil [see e.g., *Wan and Wilson*, 1994a, 1994b; *Chen and Flury*, 2005; *Gao et al*., 2006]. All these experiments were performed with air and water as the two immiscible phases. But, it is difficult to control air flow rate in a network of pores. Also, in some visualization experiments, the two fluids must have the same index of refraction; this is not possible with air and water. So in some experiments, two immiscible liquids have been employed. Moreover, colloid transport in porous media involving two liquids is important in some industrial applications. Recently, transport of colloids in oil-water system and their behavior close to the oil-water interface, were studied by *Leunissen et al*. [2007]. *Zevi et al*. [2010] employed water and low-viscosity silicone oil as the wetting and nonwetting phases to study pathogen transport during two-phase flow. *Zhang et al*. [2013] also used two liquids, namely water and fluorinert, and studied the effect of interfaces on the distribution of colloids in a PDMS micromodel.

[6] In this work, we report on results of experiments performed in a PDMS micromodel under steady-state and transient two-phase flow conditions. Our aim was to study pore-scale processes that affect the remobilization of attached colloids, when fluid saturation is changed, i.e., when imbibition or drainage occurs. In particular, we were interested in the role of fluid-fluid interfaces in the remobilization. Another objective was to formulate a macroscale model of colloid transport and remobilization and produce experimental data for verifying it. We directly observed the distribution and movement of colloids by means of a confocal microscope. We also measured the concentrations of colloids as a function of time in the outlet reservoir. We performed transport experiments under steady-state flow (of one of the phases) followed by imbibition or drainage. To simulate the remobilization of colloids, the rate of colloid detachment from solid surfaces was modeled as a linear function of the rate of change of saturation. The remobilization of colloids attached to fluid-fluid interfaces was modeled as a function of the change in interfacial area. This is the first study of colloid transport in two-phase flow, where pore-scale visualization, breakthrough concentration measurement, and modeling of results are combined. Video images, included as supporting information, provide insightful images of the movement of colloid in a network of pores occupied by two immiscible liquids.

2. Experimental Materials and Methods

[7] We have performed experiments on transport of colloids in a micromodel. The details of our experimental setup can be found in *Zhang et al*. [2013]. A schematic representation of the setup is shown in Figure 1. The micromodel pore network covered an area of 1 mm × 10 mm. It contained around 90 pore bodies and 200 pore throats, with mean pore size of 30 μm, and porosity of 40%. The micromodel ended in an outlet channel, leading to an outlet reservoir. Details of micromodel fabrication and construction were described in *Karadimitriou et al*. [2013]. To make the micromodel uniformly and stably hydrophobic, the micromodel was treated by a silanization process [see *Karadimitriou*, 2013, chap. 5]. Using a confocal microscope, images were acquired of the movement of phases and colloids within the micromodel. The microscope was also used to measure the concentration of colloids in the outlet channel, as described shortly. A dual-direction syringe pump was used to control the flow rates of liquids and colloid suspension via a three-way valve. The pump could be used to inject water (with or without colloids) or fluorinert through three different inlets of the micromodel.

[8] The two fluids in our study were fluorinert and water. We chose fluorinert instead of air, mainly because fluorinert and water have almost the same refractive indices. This is necessary for using confocal microscopy and being able to focus at different depths of the micromodel. Given the fact that the micromodel was hydrophobic, fluorinert was the wetting phase, and water was the nonwetting phase. The colloids used in this study were carboxylate-modified polystyrene fluorescent microspheres with a mean diameter of 300 nm and a particle density of 1055 kg m^{-3}. They were hydrophilic and had negatively charged

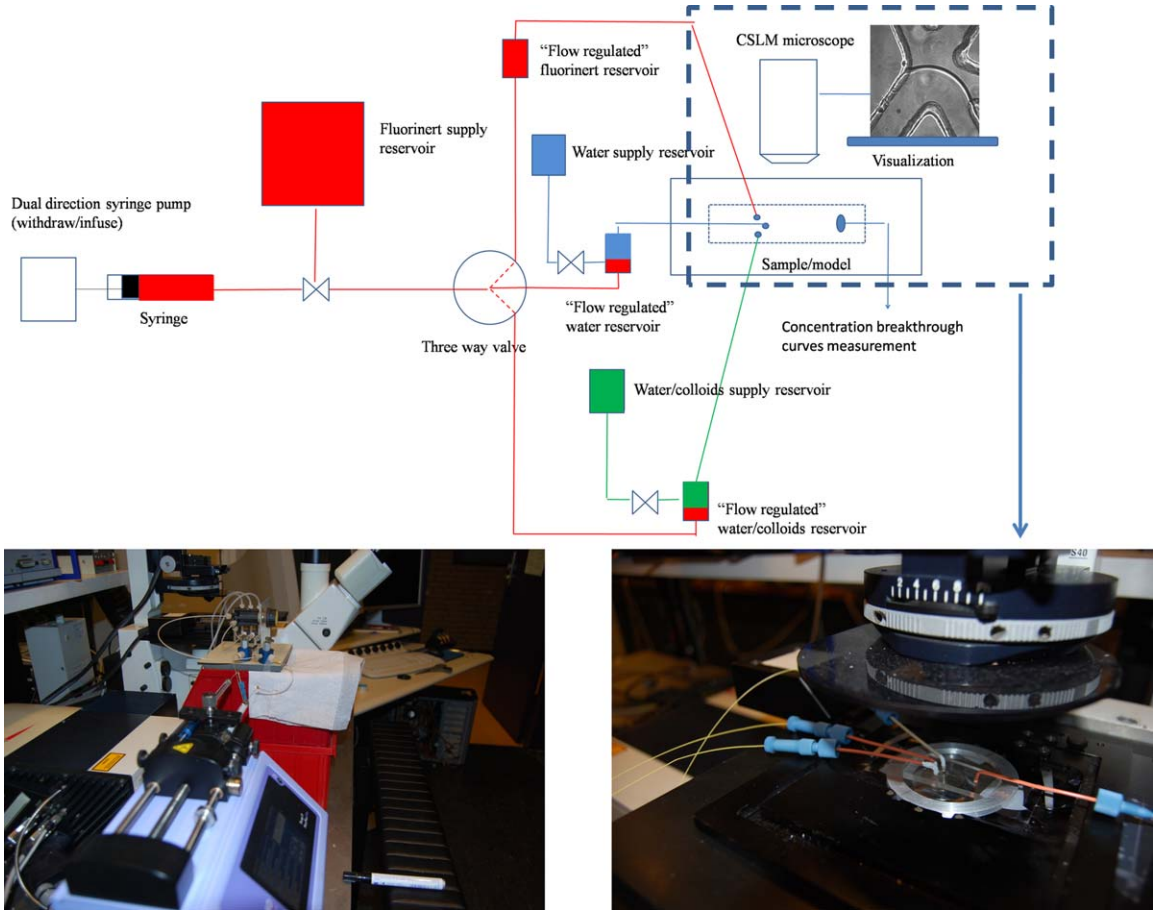

Figure 1. Schematic representation of the experimental setup.

surfaces. The colloid suspensions were prepared by dispersing the microspheres in deionized (DI) water to reach a final concentration of around 5.8×10^{10} particles/L. The pH of the suspension was measured and kept between 6.8 and 7.0 during the experiments. Also, the value of ionic strength was kept constant at 1.2×10^{-3} mM. All experimental conditions are listed in Table 1.

[9] The experiments were conducted in three stages. The ***first stage*** was designed to create steady-state flow of water at constant water saturation with no colloids. We performed experiments at three different water saturations: 100%, 60%, and 40%, denoted as experiment 1, experiment 2, and experiment 3, respectively.

[10] In order to achieve 100% water saturation, the model was put vertically and then flushed with carbon dioxide for few minutes to expel the air. After that, the micromodel was put horizontally on the stage of the confocal microscope and connected to the injection tubes. Then, DI water was introduced into the micromodel at the rate of 150 nL/min in order to displace and dissolve the carbon dioxide, leading to a fully saturated micromodel. To create steady-state unsaturated flow conditions, first the micromodel was saturated with fluorinert. Then, water was injected at a rate of either 500 nL/min or 850 nL/min to establish a water saturation of approximately 40% or 60%, respectively. We continued the flow at the corresponding rate until visualization images showed a stable flow field, where the fluid-fluid interfaces did not move anymore. In all three experiments, the micromodel was flushed under steady-state flow for approximately 5 h.

Table 1. Experimental Conditions of Micromodel Measurements

Parameter	Experiment 1	Experiment 2	Experiment 3
Flow rate during stage 1 (nL/min)—steady-state flow without colloids	150	850	500
Flow rate during stage 2 (nL/min)—steady-state flow with colloids	150	850	500
Flow rate during imbibition (nL/min)—injecting fluorinert to displace water	150	150	150
Flow rate during drainage (nL/min)—injecting more water		2500	2000
Initial water saturation (%)	100	60 (±2)	40 (±2)
Final water saturation in imbibition experiments (%)	20 (±2)	15 (±2)	20 (±2)
Final water saturation in drainage experiments (%)		80 (±5)	55 (±5)
pH	6.8	6.8	6.8

[11] The water distribution was visualized by a setup developed by *Karadimitriou et al*. [2012] and saturation as well as capillary pressure was determined using image analysis software IDL. Saturation of water was calculated as the ratio of the pixels which corresponded to the nonwetting phase (water dyed with ink), over the total number of pixels of the flow network. Average capillary pressure of the collection of all interfaces within the flow network was calculated as the average of local capillary pressures weighted with local interfacial areas. We performed separate experiments to obtain the saturation-capillary pressure curves for each micromodel.

[12] The ***second stage*** involved colloids transport under steady-state flow conditions. In both saturated and unsaturated experiments, keeping flow rate the same as during steady-state flow, the particle suspension was injected for 20 min. This was followed by the injection of colloids-free DI water for 25 min without changing the flow rates. So the second stage of experiment, i.e., colloids transport under steady-state flow, lasted for 45 min. The ***third stage*** involved transient two-phase flow and remobilization of attached colloids. This started either with injecting fluorinert (causing imbibition) to displace the water phase and reduce its saturation; or increasing the flow rate of water to increase its saturation (causing drainage).

[13] During the experiments, colloids distribution and their interactions with solid-water interfaces (SWIs), fluorinert-water interfaces (FWIs), and fluorinert-water-solid contact lines (FWSCs) within the flow network were directly observed by confocal microscopy. In addition to still images, real-time images were also taken for subsequent review and analysis of colloids interactions with the moving interfaces and contact lines. All experiments were repeated, and fluids distribution was found reproducible. Then the experiments were repeated under the same conditions as visualization experiments, but this time the confocal microscope was used to measure concentration in the outlet channel as a function of time. The measured breakthrough curves were reproducible too. The concentration was determined by measuring the fluorescence intensity of particles at a focus surface (in the horizontal middle plane) of the micromodel outlet channel at a speed of 834 ms/frame. Colloids above and below this focus surface were out of confocal focus, but we assumed the colloids distribution was uniform over the depth. First a calibration curve was prepared by injecting known concentrations of water-colloid suspension into the outlet channel of the micromodel via the outlet reservoir. By measuring the fluorescence intensity of various known concentrations, the calibration curve was obtained. The confocal images were all taken at low intensities (<100 μW) to avoid bleaching of the fluorescent dye.

3. Mathematical Model

[14] For modeling the experiments, two-phase flow equations as well as colloid transport equations were employed and solved numerically.

3.1. Flow Equations

[15] We assumed that the solid phase is rigid and the fluid phases are incompressible. Thus, the combination of mass balance equations and Darcy's law led to the following set of governing equations for fluorinert and water

$$\phi \frac{\partial S_f}{\partial t} + \nabla \cdot \left(\frac{K k_{rf}}{\mu_f} \nabla P_f \right) = 0 \tag{1}$$

$$-\phi \frac{\partial S_f}{\partial t} + \nabla \cdot \left(\frac{K k_{rw}}{\mu_w} \nabla P_w \right) = 0 \tag{2}$$

where subscripts f and w indicate fluorinert and water (wetting and the nonwetting phase, respectively), ϕ is the porosity; S_α is the α-phase saturation; K is the intrinsic permeability [L^2]; $k_{r\alpha}$ is the α-phase relative permeability; μ_α is the dynamic viscosity [M L^{-1} T^{-1}]; and P_α is the α-phase pressure [M T^{-2} L^{-1}]. Because the micromodel was put horizontally on the stage of the microscope, we did not consider gravity.

[16] We also employed the following constitutive equations for relative permeability and capillary pressure [*Mualem*, 1976; *van Genuchten*, 1980]

$$k_{rf} = S_e \left[1 - \left(1 - S_e^{\frac{1}{m}} \right)^m \right]^2 \tag{3}$$

$$k_{rw} = (1 - S_e)^{1/2} \left(1 - S_e^{1/m} \right)^{2m} \tag{4}$$

$$P_w - P_f = P_c(S) = \frac{1}{\alpha} \left(S_e^{-1/m} - 1 \right)^{1/n} \tag{5}$$

where $m = 1 - 1/n$ is the parameter n can be related to the pore size distribution, α [Pa^{-1}] can be interpreted as the inverse of the entry pressure, S_e is the effective saturation, defined as $S_e = (S_f - S_{rf})/(1 - S_{rf})$, where $S_{rf} \leq S_f \leq 1$.

[17] The initial condition for each experiment was set to the specified saturation given in Table 1 and the corresponding pressure. For the inlet boundary condition, we specified the flux of the nonwetting phase (water) for drainage experiments and the flux of the wetting phase (fluorinert) for imbibition experiments. The outlet boundary pressure was set equal to zero.

3.2. Transport Equations

[18] We simulated colloid transport during stages 2 and 3 by advection-dispersion-sorption equations. As the colloids were hydrophilic, they were present in the water (i.e., the nonwetting phase) only. The governing equation for colloids transport in the water phase is

$$\phi \frac{\partial S_w C_w}{\partial t} = \frac{\partial}{\partial x} \left(\phi S_w D \frac{\partial C_w}{\partial x} \right) - \frac{\partial q_w C_w}{\partial x} - \gamma_s - \gamma_{fw} \tag{6}$$

where C_w [Number L^{-3}] is the number concentration of colloids in water (number of colloids per unit volume of water), D [L^2 T^{-1}] is the dispersion coefficient, q_w [L T^{-1}] is the flow rate, γ_s and γ_{fw} [Number L^{-3} T^{-1}] are net rates of attachment of colloids to SWIs and FWIs, respectively. The net rate of attachment to FWIs can be expressed as

$$\gamma_{fw} = \frac{\partial a_{fw} C_{fw}}{\partial t} \tag{7}$$

where a_{fw} [L^{-1}] is the specific fluorinert-water interfacial area per unit volume of porous medium; C_{fw} [Number L^{-2}] is the concentration of colloids attached to the FWI given as

the number of colloids per unit area of fluorinert-water interface. According to the theory developed by *Hassanizadeh and Gray* [1993], interfacial area depends not only on saturation but also on capillary pressure. However, for the purpose of this study, we assumed that a_{fw} only depends on saturation. This is certainly justified in the case of imbibition experiments, where the primary imbibition curve was followed, along which there is unique relationship between saturation and capillary pressure. Here we used the following formula for a_{fw} [*Karadimitriou*, 2013]

$$a_{fw}=a_0(1-S_w)^{1.2}S_w \tag{8}$$

where a_0 is the specific interfacial area corresponding to residual saturation of the medium.

[19] In principle, FWI colloid attachment/detachment should be modeled as a kinetic process. But in our preliminary simulations, we found that the kinetic constant is large and an equilibrium description provides satisfactory results. This was in line with our findings when we simulated the experimental results of *Torkzaban et al*. [2006a, 2006b] [see *Zhang et al*., 2012].

[20] Therefore, we assumed a linear equilibrium partitioning of colloids between water and fluorinert-water interface, such that

$$C_{fw}=K_D^a C_w \tag{9}$$

where K_D^a [L] is the equilibrium distribution coefficient for attachment to the FWI. Note that equations (7) and (9) model both attachment of colloids to FWIs and their remobilization. When fluorinert-water interfaces are created (which occurs mainly during drainage), more colloids can get attached to them. But, when interfaces are destroyed (which occurs mainly during imbibition), attached colloids are released back into the water phase.

[21] The attachment/detachment to/from SWI is described by the following equation [due to *Cheng and Saiers*, 2009]:

$$\gamma_s=\frac{\partial \rho_b C_s}{\partial t}=\phi S_w k_{att}^s C_w-(1-\phi)\rho_s k_{det}^s C_s-(1-\phi)\rho_s\sum_{i=1}^{N_c}k_{rem}^i(t)C_{si} \tag{10}$$

where C_s [M^{-1}] is the number of colloids attached to the SWI per unit mass of solid phase; ρ_s [$M\ L^{-3}$] is the mass density of the PDMS solid grain; k_{att}^s and k_{det}^s [T^{-1}] are the attachment and detachment rate coefficients of colloids to and from the solid-water interface, respectively. The last term in equation (10) models the colloids remobilization from SWI due to transient flow. The time-dependent coefficient $k_{rem}^i(t)$ and N_c are defined shortly. Note that the last term will be nonzero only in stage 3 of the experiments, i.e., during transient conditions.

[22] For stage 2 (steady-state flow), the initial conditions were $C_w(x, 0) = 0$ and $C_s(x, 0) = 0$. The inlet boundary conditions were $C_w(0, t) = C_0$ ($0<t<t_{seeding}$) and $C_w(0, t) = 0$ ($t_{seeding}<t<t_{end}$), where $t_{seeding}$ represents the final time of colloids seeding and t_{end} is the final time of steady-state transport. For the outlet boundary, a zero concentration gradient was assumed.

[23] For stage 3 of the experiments, the inlet boundary condition was zero concentration, and for the outlet boundary, a zero dispersion flux was imposed. The initial conditions were $C_w(x, 0) = C_{w0}(x)$ and $C_s(x, 0) = C_{s0}(x)$, where C_{w0} and C_{s0} are given by the profiles of the colloid concentration in water and attached to SWIs, respectively. These profiles were obtained from the distribution at the final time of stage 2.

[24] Following *Cheng and Saiers* [2009], the remobilization coefficient $k_{rem}^i(t)$ is assumed to be related to the time rate of change of saturation. *Cheng and Saiers* [2009] hypothesized that remobilization of attached particles occurs only in pores that are being emptied during drainage or are filled during imbibition. Based on the variability in pore size, the pores were divided into N_c compartments. Once a compartment i empties or fills as its entry pressure P_{ci} is reached, attached particles are assumed to be removed from the pore walls of that compartment. Thus, the remobilization coefficient for imbibition and drainage is given by the following equations, respectively.

$$k_{rem}^i(t)=\begin{cases}0 & for \quad P_w-P_f>P_{ci}\\ N_{imb}\left|\dfrac{\partial S_w}{\partial t}\right| & for \quad P_w-P_f\le P_{ci}\end{cases} \tag{11}$$

$$k_{rem}^i(t)=\begin{cases}0 & for \quad P_w-P_f<P_{ci}\\ N_{dr}\left|\dfrac{\partial S_w}{\partial t}\right| & for \quad P_w-P_f\ge P_{ci}\end{cases} \tag{12}$$

where P_w and P_f are the fluid pressures obtained by solving equations (1–5); P_{ci} is the entry pressure for each compartment i; N_{imb} and N_{dr} are the empirical coefficients that quantify colloids remobilization during imbibition and drainage, respectively. The entry pressure for each compartment was determined from the capillary pressure-saturation curve.

[25] The set of equations presented above were solved with the aid of COMSOL 4.3a. The model was coupled to the genetic algorithm [see *Houck et al*., 1995] optimization module in MATLAB in order to determine model parameter values. All model parameter values are given in Table 2.

4. Results

4.1. Colloids Transport and Retention Under Steady-State Flow

[26] As mentioned earlier, colloid transport experiments during steady-state flow were performed at three different water saturations: 100%, 60%, and 40%. The seeding lasted 20 min followed by 25 min of steady-state colloids-free water flow. The measured breakthrough curves are shown in Figure 2. It is clear that there was significantly more retention at lower water saturations. The peak values of normalized breakthrough concentrations are around 0.95, 0.80, and 0.65 for experiments 1, 2, and 3, respectively. Also, the total mass recovered at the end of stage 2, given in Table 3, was less at a lower saturation. Pore-scale images with the size of 512 μm × 512 μm, taken with confocal microscope from an area at the middle plane of the micromodel (the same depth where the breakthrough concentrations were measured), helped us to see colloid

Table 2. Parameters Determined From Fitting the Breakthrough Curves (Average ± Standard Deviations)

	Parameter	Experiment 1	Experiment 2	Experiment 3
Steady-state condition	Dispersivity (cm)	0.035	0.052	0.09
	SWI attachment coefficient, k^s_{att} (s^{-1})	1.07 (±0.096) × 10^{-3}	1.63 (±0.12) × 10^{-3}	1.58 (±0.14) × 10^{-3}
	SWI detachment coefficient, k^s_{det} (s^{-1})	0.1117 (±0.006) × 10^{-3}	0.17 (±0.005) × 10^{-3}	0.2167 (±0.017) × 10^{-3}
	K^a_D (m)		0.75 (±0.1)	0.57 (±0.02)
Transient condition (imbibition and drainage)	N_{imb}	1.53	0.32	0.26
	a_0 (m^{-1})	2500	2500	2500
	α (m^{-1})	0.000395	0.000395	0.000395
	N	5.17	5.17	5.17
	N_c	5	5	5
	N_{dr}		0	0

attachment sites. An example is shown in Figure 3. The particles observed in this image are either in water or attached to the FWIs and FWSCs. There are also few colloids attached to SWIs.

4.2. Remobilization of Colloids During Imbibition

[27] As mentioned earlier, the seeding of colloids during steady-state water flow (stage 2) was followed by transient flow, basically changing the saturation (stage 3). In the case of imbibition, this was achieved by stopping the flow of water and injecting fluorinert at a rate of 150 nL/min. This resulted in a sudden decrease of water saturation to the residual value in all three experiments. When fluorinert was observed coming out of the outlet reservoir, then we stopped the experiments. The imbibition process caused a remobilization of the colloids that were left in the micromodel at the end of stage 2. The remobilization of colloids resulted in a spike in the breakthrough concentration as can be seen in Figure 2. The peak concentration is highest for experiment 1 and lowest for experiment 3. The strength of this remobilization (the peak concentration) depends on two main factors: (1) the rate of saturation change (which was a reduction from 100% to 20%, from 60% to 15%, and from 40% to 20% in experiments 1, 2, and 3, respectively, in increasingly longer times); (2) the accessibility of emplaced colloids to the displacing fluorinert. In the case of saturated experiments, much more water (and thus colloids) was displaced during imbibition stage than in the unsaturated experiments. That is why the peak in experiment 1 was the highest. The amount of colloids remobilized during this peak was very significant (see Table 3). The ratios of remobilized colloids to the total remaining at the end of stage 2 were 8.3%, 21.3%, and 11.3%, respectively.

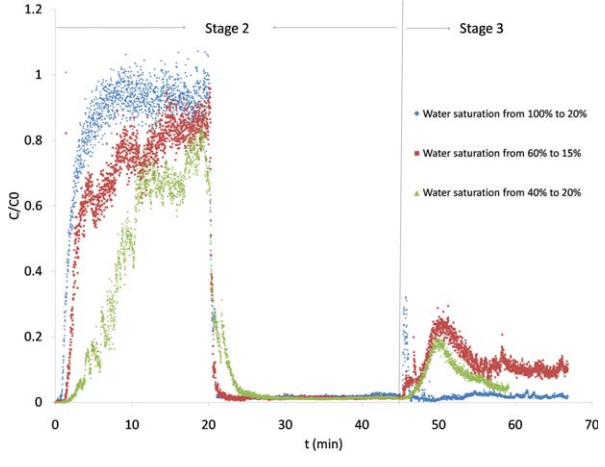

Figure 2. Breakthrough curves measured in the outflow reservoir, showing the impact of saturation on the transport and remobilization of colloids under steady-state flow (stage 2) and during imbibition (stage 3).

[28] Real-time images of the movement of colloids can be found in supporting information (see Movie 1 and Movie 2). Four images from experiment 2 (with initial water saturation of 60%) are shown in Figure 4. The images show that as the imbibition front advanced into the micromodel, FWIs, and FWSCs, and colloids attached to them, were pushed toward the outlet. Moreover, the moving FWIs and FWSCs scoured the colloids attached to the solid surface. We know that some of these colloids re-entered the flowing water. This was the case with "interface 1" shown in Figure 4.

[29] During imbibition, we also had local drainage. For example, we can see that water is pushed into large pore B (see Figure 4a) displacing fluorinert. The interface corresponding to this local drainage is interface 2. Some of the colloids attached to interface 2 were redeposited on the SWI in pore B, as visible in areas indicated by white circles in Figures 4c and 4d. Some of the remobilized colloids originated from immobile water blubs that were trapped in the pore network and got reconnected during imbibition and moved out of the network. But due to the limitations of the objective lens, we could not capture this phenomenon.

4.3. Colloids Transport During Drainage

[30] In the case of experiments 2 and 3 (with a water saturation of 60% and 40%, respectively), we also performed

Table 3. Calculated Colloid Mass Recovered in the Micromodel Effluent

	Mass Balance (%)		
		Remobilized During Imbibition Spike	
Experiment Number	Remaining at the End of Stage 2	% of Total Injected Colloids	% of Remaining of Stage 2
Experiment 1	12 (±2)	1 (±0.1)	8.3
Experiment 2	30 (±4)	6.4 (±0.4)	21.3
Experiment 3	47 (±5)	5.3 (±0.2)	11.3

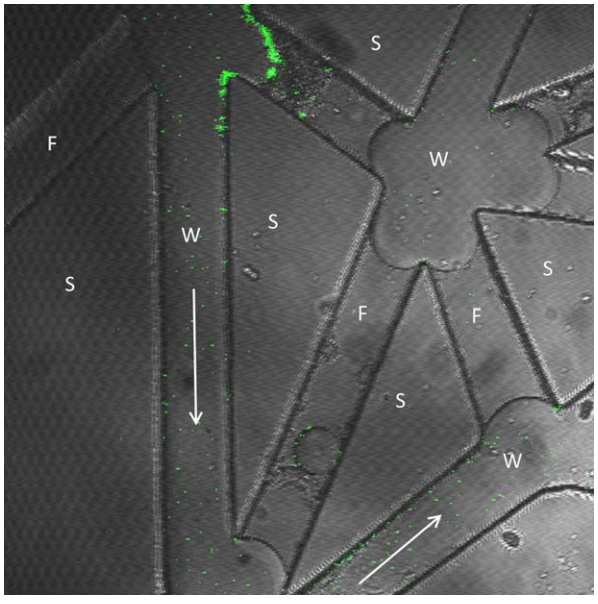

Figure 3. A confocal microscope image of micromodel (image size 512 μm $\times$ 512 μm) during unsaturated steady-state flow: S, PDMS solid; W, water; and F, fluorinert. White arrows indicate the flow path and direction. Green dots are colloidal hydrophilic particles.

drainage experiments; i.e., we expelled fluorinert and increased water saturation. This was achieved by increasing the flow rate of fresh water by a factor of four. The measured breakthrough concentration curves are shown in Figure 6. Real-time images of parts of micromodel are also shown in Movie 3 and Movie 4 of supporting information.

[31] Contrary to the case of imbibition, we did not find any peak in the breakthrough curves, which means no remobilization, occurred during drainage. The main reason for the lack of remobilization in our drainage experiments is that FWIs and FWSCs moved very little and the distribution of water and fluorinert did not change much. Because the micromodel was fluorinert-wet, despite the fourfold increase in water injection rate, the water saturation change was small: from 60% to 80% and from 40% to 55% in experiments 2 and 3, respectively. From the real-time images shown in Movie 3 and Movie 4 of supporting information, we can see that even some FWIs were destroyed as water pockets get reconnected; the released colloids got attached to other FWIs downstream. In fact, drainage (i.e., the increase of water saturation in our case) generally leads to an increase in fluid-fluid interfacial area [see e.g., *Karadimitriou et al*., 2013]. So there is no decrease in the number of attachment sites in our drainage experiments, and therefore no remobilization.

4.4. Simulation of Breakthrough Curves

[32] Experimental results were simulated based on the model presented earlier in this paper. For the stage 2 of experiments, only colloid transport equations had to be solved as the flow velocity was known and constant. Data from the stage 2 were used to determine the values of attachment and detachment coefficients k^s_{att} and k^s_{det} (for solid phase) as well as the distribution coefficient K^a_D (for FWI). The fitted values are given in Table 2. As we can see, the value of attachment coefficient, k^s_{att}, is larger for experiments with smaller water saturation. The value of detachment coefficient, k^s_{det}, is 1 order of magnitude smaller than the attachment coefficient. Also, it does not show a clear correlation with saturation. The values of the FWI distribution coefficient K^a_D are the same for stage 2 and stage 3. This is to be expected as this coefficient accounts for local equilibrium between colloids in water and attached to interfaces; so it should be independent of saturation.

[33] For stage 3 of experiments (transient flow), flow equations were solved too. Parameter values determined from steady-state experiment were kept unchanged for the transient part. Results of simulation of the three imbibition experiments are shown in Figure 5, and for the two drainage experiments, they are given in Figures 6a and 6b. The agreement between simulations and data is very good. In particular, it is encouraging that the remobilization parts of the curves are closely followed by the simulations.

5. Discussion and Conclusions

[34] In this study, we employed three approaches to investigate colloid transport and in particular the remobilization of colloids under transient two-phase flow conditions in a porous medium. The first approach was pore-scale visualization using a confocal laser microscope, which allowed direct observation of movement of colloids and fluid-fluid interfaces. Due to the limitation of the objective lens of confocal microscope, we could monitor only a few pores in a single image at any given time. Nevertheless, the visualization gives us valuable insight in attachment as well as remobilization mechanisms as interactions of colloids with fluid-fluid and fluid-solid interfaces can be directly observed. The second approach was the measurement of the effluent concentration, which provided quantitative information on the macroscale behavior of the colloid transport through the micromodel.

[35] Our third approach was the numerical simulation of the breakthrough curves. For describing the remobilization of colloids as a result of saturation change, we adapted the remobilization model of *Cheng and Saiers* [2009]. They assumed that the colloid remobilization occurs only in pores where fluid saturation changes drastically, for example due to snap-off. This means that the remobilization starts in larger pores during drainage (and then in a hierarchy of smaller and smaller pores), but it starts in smaller pores during imbibition (and then in a hierarchy of larger and larger pores). *Cheng and Saiers* [2009] did not explicitly model colloid attachment/detachment related to fluid-fluid interfaces. They lumped it into the attachment/detachment processes at solid-wetting phase interface. We used Cheng and Saier's model to describe colloid release from solid surfaces, but we explicitly accounted for fluid-fluid interfaces and corresponding attachment and remobilization. Moreover, we did not explicitly model the evolution of interfaces with time. Instead, we assumed that the fluid-fluid interfacial area is a function of saturation. This assumption is valid during the primary imbibition process. Through visualization experiments, we clearly observed colloids attached to the FWSCs. But, in the simulation, we

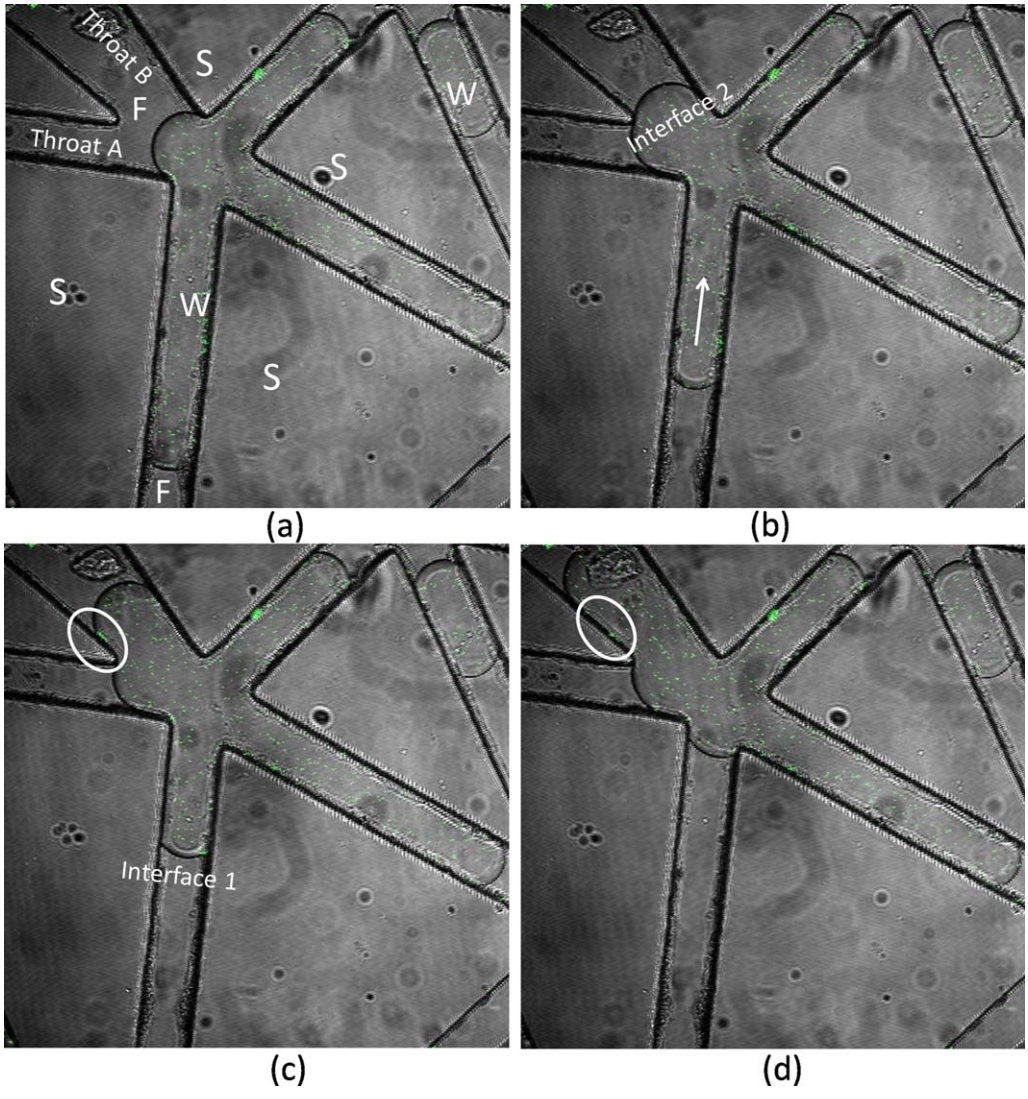

Figure 4. Real-time images of colloids transport during imbibition in stage 3 of experiment 2 (initial water saturation of 60%). Times are given from the start of stage 2 (see also Figure 1). (a) Right before the start of imbibition, $t = 45$ min; (b) $t = 45$ min 16 s; (c) $t = 45$ min 31 s; and (d) $t = 46$ min 22 s. Arrow shows the direction of the flow: S, PDMS matrix; F, fluorinert; and W, water.

did not explicitly model colloids attached to/detached from FWSC; this effect was lumped into attachment to SWI.

[36] Similar models, accounting for attachment of colloids to fluid-fluid interfaces were proposed by *Schfifer et al*. [1998], *Šimůnek et al*. [2006], and *Kim et al*. [2008]. They modeled colloid accumulation to fluid-fluid interfaces depending on the varying specific fluid-fluid interfacial area. In all three cases, they studied colloid transport under steady-state flow conditions; so no remobilization was considered.

[37] Our micromodel was hydrophobic which means that water was the nonwetting phase and fluorinert was the wetting phase. The colloids were hydrophilic and could not disperse in fluorinert. So our experiments would be similar to the transport of colloids in a hydrophobic soil. Therefore, a direct application of our results to natural soil is not possible. But we can learn about the role of fluid-fluid interfaces and the effect of change in water saturation on colloids behavior.

[38] Our results clearly show a very significant increase in colloids removal during steady-state flow under unsaturated conditions compared to saturated conditions. It must be noted that the flow rate in all experiments was the same. So the average pore velocity was higher in unsaturated experiments. Higher velocities should lead to less attachment. Yet we had more attachment under unsaturated conditions. After injecting a pulse of colloids, 88% of colloids were found in the effluent of the water-saturated micromodel as opposed to 70% and 53% when the micromodel saturation was 60% and 40%, respectively.

[39] The enhanced removal of colloids under unsaturated conditions has been reported by many researchers. Various authors have mentioned (a combination of) different mechanisms for this enhanced attachment. For example,

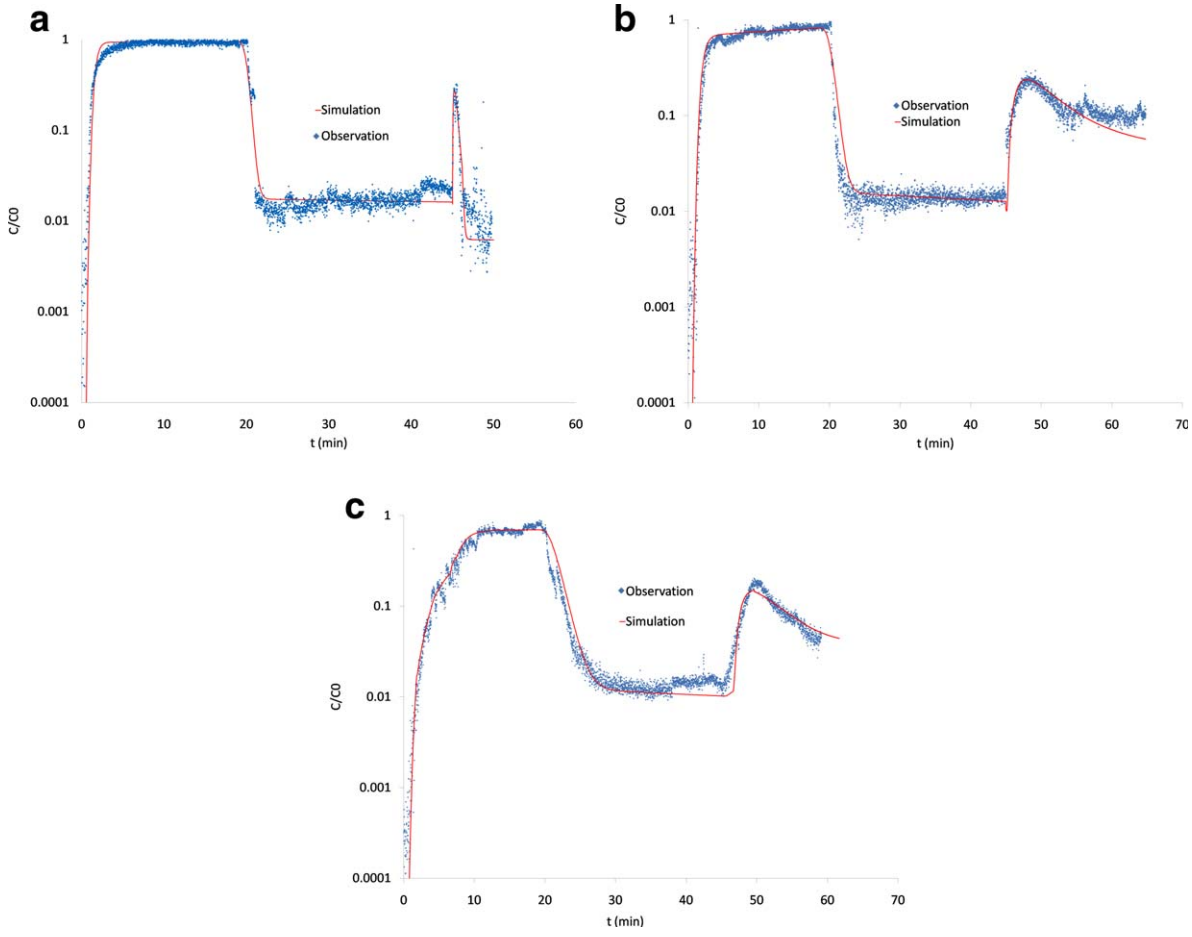

Figure 5. Measured (dots) and fitted (line) breakthrough curves of (a) experiment 1 (from water saturation 100% to 20%), (b) experiment 2 (from 60% to 15%), and (c) experiment 3 (from 40% to 20%).

Torkzaban et al. [2006a] reported that there is enhanced adsorption of viruses to the solid-water interface. The explanation for this mechanism is as follows. Under unsaturated conditions, the thickness of a water pathway becomes smaller because the pore space is shared by water and fluorinert. Thus, the colloids have to travel closer to the pore walls and they have a higher chance of getting attached. This mechanism could not occur in our

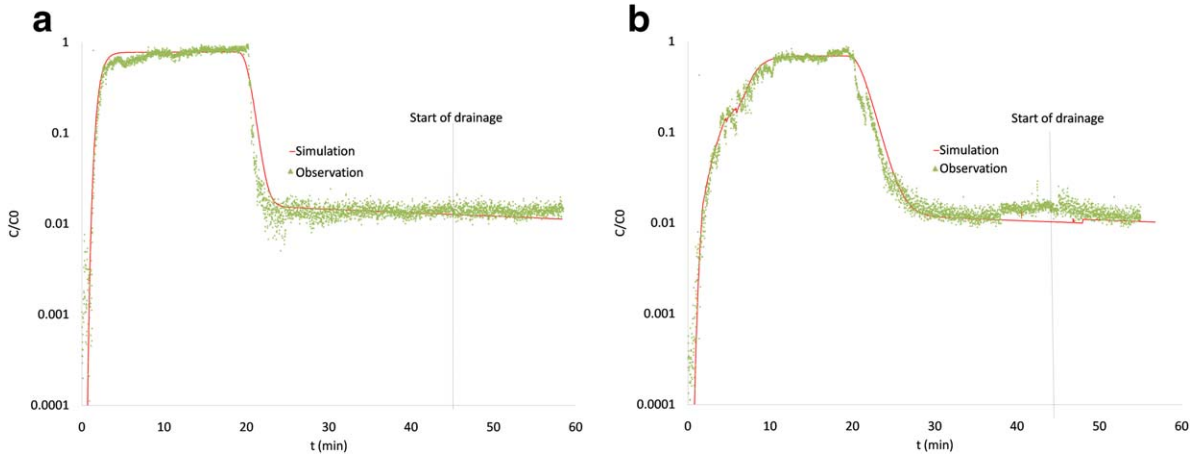

Figure 6. Breakthrough curves of (a) experiment 2 (drainage causing increase of water saturation from 60% to 80%) and (b) experiment 3 (drainage causing increase of water saturation from 40% to 55%). Measured data are shown as dots and simulation results are shown as solid lines. Note that the steady-state flow parts of the curves are identical to the results shown in Figure 2.

micromodels and we did not find enhanced attachment to the solid phase. When comparing images from saturated and unsaturated experiments, we did not find observable differences in the number of colloids attached to the solid-water interface. In fact, in our micromodel, at any given location, the pore space was not being shared by the two fluids. Any given pore segment was filled either by water or by fluorinert. So the thickness of a pathway filled by the wetting phase was not different under different saturations. Second, our numerical simulation results did not show a significant increase of attachment to the solid phase. The estimated values of attachment and detachment coefficients are given in Table 2. We see that the values of the ratio of k^s_{att}/k^s_{det} for the three experiments are not drastically different. It could be that we did not see a significant increase in attachment because the colloids were dispersed in water, which was the nonwetting phase in our micromodel.

[40] Another mechanism for enhanced attachment under unsaturated conditions is reported to be attachment to fluid-fluid interfaces [e.g., *Wan and Wilson*, 1994a, 1994b; *Powelson and Mills*, 2001; *Keller and Sirivithayapakorn*, 2004; *Torkzaban et al*., 2006a, 2006b] and fluid-fluid-solid contact lines [see e.g., *Crist et al*., 2004, 2005; *Zevi et al*., 2009]. This seems indeed to be the main mechanism for enhanced attachment according to our experimental results. We certainly observed a large number of colloids attached to FWIs and FWSCs. Also, we clearly had more interfaces and contact lines at lower saturations. So even if the attachment per surface area of interface was constant, there was more attachment at lower saturations. For a satisfactory simulation of breakthrough curves, we needed to include the attachment of colloids to interfaces and contact lines.

[41] Finally, a third mechanism for enhanced attachment is reported to be the straining of colloids by thin films of water [see e.g., *Wan and Tokunaga*, 1997; *Auset et al*., 2005]. We could not investigate this effect in our experiments. First of all, the wetting phase (that could form a film) was fluorinert in our case. But, fluorinert was devoid of colloids. So colloids could not be trapped in such films. Second, wetting phase films are expected to be a few nanometers thick and the objective lens of our microscope was not able to see such a thin film.

[42] We also performed transient experiments to investigate the effect of saturation change on remobilization of attached colloids. We performed both imbibition and drainage experiments, starting from different initial saturations. Before transient experiments, a pulse of colloids were injected (during steady-state flow) in order to emplace colloids in the micromodel. Both pore-scale images and breakthrough curves showed a significant remobilization of colloids occurring during imbibition (i.e., fluorinert displacing water, which contained colloids). As can be seen in Movie 1 and Movie 2, as soon as fluorinert started to displace water, FWI interfaces, with colloids attached to them, were pushed toward the micromodel outlet. Moving interfaces also scoured colloids attached to the solid surface. In the breakthrough curve, we see a distinct spike in concentration. The peak concentration was largest for the experiment 1, where the water saturation dropped from 100% to about 20% in a short time. This was a saturation change of 80%. A lower peak concentration was observed in experiment 2, where the water saturation was reduced from 70% to 15% (giving a saturation change of 55%). The lowest peak concentration was reached in experiment 3, where the water saturation changed only 20% (from 40% to 20%). So clearly the strength of remobilization depends on the degree of saturation change. At the same time, a reduction of the water saturation leads to the creation of more fluid-fluid interfaces. So remobilized colloids could reattach to new FWIs. This is why the overall percentage of emplaced colloids that were remobilized is lower in the case of experiment 1 (see Table 3) as many new interfaces were created in that case.

[43] We also performed drainage experiments, where water saturation was increased from an initial value of 60% to 80% in experiment 2 and from 40% to 55% in experiment 3. Contrary to imbibition experiments, we found no remobilization of attached colloids. The main reason for this result is that the saturation change, and thus the change in fluids distribution, was small. This also meant that there was not much change in amount of interfacial area. So the water flow field did not change much before and after drainage. Another reason is that there were no colloids available in the fluorinert to be remobilized.

[44] The main forces that control the remobilization of attached colloids due to saturation change are DLVO forces as well as hydrodynamic and capillary forces. Colloids are subject to forces and torque due to water flow, as well as surface tension when touched by a fluid-fluid interface. These nonDLVO forces are likely to play a significant role under unsaturated conditions. *Bradford and Torkzaban* [2008] have reported that capillary forces can be several orders of magnitude bigger than DLVO force and hydrodynamic force. The capillary forces help pin the colloid at the FWSC and FWI. Under transient unsaturated conditions, the colloids attached to the solid surface can be dislodged by a moving FWI and/or FWSC due the pulling of capillary forces, leading to colloid remobilization. The force balance is described by *Shang et al*. [2008, 2009] in detail, which calculated and directly measured forces exerting on colloids, and suggested that capillary forces play the dominant role in controlling colloid remobilization.

[45] Our results are only partially comparable to the studies reported in the literature. Some studies have shown that remobilization occurs during both drainage and imbibition [*Saiers et al*., 2003; *Zhuang et al*., 2007; *Cheng and Saiers*, 2009], even with a stronger remobilization during drainage [*Cheng and Saiers*, 2009]. But, these drainage experiments involved displacement of the wetting phase (which was water containing colloids) by air (the nonwetting phase). In our case, drainage means the displacement of fluorinert (which has no colloids) by water (injected without colloids). So if the injected fresh water does not disturb the residual water much, we should not find remobilization, as observed in our experiments.

[46] In summary, our experiments show that micromodel experiments combined with confocal laser microscopy provides valuable insights in the behavior of colloids in porous media filled by two fluid phases. Fluid-fluid interfaces and fluid-fluid-solid contact lines play a major role in the retention as well as remobilization of colloids. So any quantitative modeling of colloid transport under unsaturated conditions must include modeling of interfaces (and preferably contact lines) and their effects on the colloids.

[47] **Acknowledgments.** Jack F. Schijven (National Institute of Public Health and the Environment, Netherlands) and Qin Chaozhong (Utrecht University, Netherlands) are gratefully acknowledged for very helpful discussions. The first author was funded by the China Scholarship Council. The first four authors are members of the International Research Training Group NUPUS, financed by the German Research Foundation (DFG) and Netherlands Organization for Scientific Research (NWO). Careful and comprehensive review by the Associate Editor and three referees, among them S. Torkzaban, which led to significant improvements of the manuscript, are greatly appreciated.

References

Aramrak, S., M. Flury, and J. B. Harsh (2011), Detachment of deposited colloids by advancing and receding air-water interfaces, *Langmuir*, *27*, 9985–9993.

Auset, M., A. A. Keller, F. Brissaud, and V. Lazarova (2005), Intermittent filtration of bacteria and colloids in porous media, *Water Resour. Res.*, *41*, W09408, doi:10.1029/2004WR003611.

Bradford, S. A., and H. Kim (2012), Causes and implications of colloid and microorganisms retention hysteresis, *J. Contam. Hydrol.*, *138–139*, 83–92, doi:10.1016/j.jconhyd.2012.06.007.

Bradford, S. A., and S. Torkzaban (2008), Colloid transport and retention in unsaturated porous media: A review of interface-, collector-, and pore-scale processes and models, *Vadose Zone J.*, *7*, 667–681.

Bradford, S. A., S. Torkzaban, H. Kim, and J. Simunek (2012), Modeling colloid and microorganism transport and release with transients in solution ionic strength, *Water Resour. Res.*, *48*, W09509, doi:10.1029/2012WR012468.

Chen, G., and M. Flury (2005), Retention of mineral colloids in unsaturated porous media as related to their surface properties, *Colloids Surf. A*, *256*, 207–216.

Cheng, T., and J. E. Saiers (2009), Mobilization and transport of in situ colloids during drainage and imbibition of partially saturated porous media, *Water Resour. Res.*, *45*, W08414, doi:10.1029/2008WR007494.

Crist, J. T., J. F. McCarthy, Y. Zevi, P. Baveye, J. A. Throop, and T. S. Steenhuis (2004), Pore-scale visualization of colloid transport and retention in partly saturated porous media, *Vadose Zone J.*, *3*, 444–450.

Crist, J. T., Y. Zevi, J. F. McCarthy, J. A. Troop, and T. S. Steenhuis (2005), Transport and retention mechanisms of colloids in partially saturated porous media, *Vadose Zone J.*, *4*, 184–195.

Flury, M., J. B. Harsh, and J. B. Mathison (2003), Miscible displacement of salinity fronts: Implications for colloid mobilization, *Water Resour. Res.*, *39*(12), 1373, doi:10.1029/2003WR002491.

Gao, B., J. E. Saiers, and J. N. Ryan (2006), Pore-scale mechanisms of colloid deposition and mobilization during steady and transient flow through unsaturated granular media, *Water Resour. Res.*, *42*, W01410, doi:10.1029/2005WR004233.

Hassanizadeh, S. M., and W. G. Gray (1993), Thermodynamic basis of capillary pressure in porous media, *Water Resour. Res.*, *29*, 3389–3405, doi:10.1029/93WR01495.

Houck, C. R., J. A. Joines, and M. G. Kay (1995), A genetic algorithm for function optimization: A Matlab implementation, *Tech. Rep. NCSU-IE-TR-95-09*, N. C. State Univ., Raleigh.

Karadimitriou, N. K. (2013), Two-phase flow experimental studies in micro-models, PhD thesis, Dep. of Earth Sci., Utrecht, Utrecht Univ., Netherlands.

Karadimitriou, N. K., V. Joekar-Niasar, S. M. Hassanizadeh, P. J. Kleingeld, and L. J. Pyrak-Nolte (2012), A new micro-model experimental approach for two-phase flow studies: Comparison with a pore-network model, *Lab Chip*, *12*, 3413–3418, doi:10.1039/C2LC40530J.

Karadimitriou, N. K., M. Musterd, P. J. Kleingeld, M. T. Kreutzer, S. M. Hassanizadeh, and V. Joekar-Niasar (2013), On the fabrication of PDMS micro-models by rapid prototyping, and their use in two-phase flow studies, *Water Resour. Res.*, *49*, 2056–2067, doi:10.1002/wrcr.20196.

Keller, A. A., and S. Sirivithayapakorn (2004), Transport of colloids in unsaturated porous media: Explaining large-scale behavior based on pore-scale mechanisms, *Water Resour. Res.*, *40*, W12403, doi:10.1029/2004WR003315.

Kim, M.-K., S.-B. Kim, and S.-J. Park (2008), Bacteria transport in an unsaturated porous media: Incorporation of air-water interfacial area into transport modelling, *Hydrol. Processes*, *22*, 2370–2376.

Lazouskaya, V., and Y. Jin (2008), Colloid retention at air-water interface in a capillary channel, *Colloids Surf. A*, *325*, 141–151.

Leunissen, M. E., A. van Blaaderen, A. D. Hollingsworth, M. T. Sullivan, and P. M. Chaikin (2007), Electrostatics at the oil-water interface, stability, and order in emulsions and colloids, *Proc. Natl. Acad. Sci. U. S. A.*, *8*, 2585–2590, doi:www.pnas.org_cgi_doi_10.1073_pnas.0610589104.

Mualem, Y. (1976), A new model for predicting the hydraulic conductivity of unsaturated porous media, *Water Res. Res.*, *12*(3), 513–522.

Powelson, D. K., and A. L. Mills (2001), Transport of Escherichia coli in sand columns with constant and changing water content water saturations, *J. Environ. Qual.*, *30*(1), 238–245.

Sadeghi, G., J. F. Schijven, T. Behrends, S. M. Hassanizadeh, J. Gerritse, and P. J. Kleingeld (2011), Systematic study of effects of pH and ionic strength on attachment of phage PRD1, *Ground Water*, *49*, 12–19, doi:10.1111/j.1745–6584.2010.00767.x.

Sadeghi, G., T. Behrends, J. F. Schijven, and S. M. Hassanizadeh (2013), Effect of dissolved calcium on the removal of bacteriophage PRD1 during soil passage: The role of double-layer interactions, *J. Contam. Hydrol.*, *144*(1), 78–87, doi:10.1016/j.jconhyd.2012.10.006.

Saiers, J. E., and J. J. Lenhart (2003), Colloid mobilization and transport within unsaturated porous media under transient-flow conditions, *Water Resour. Res.*, *39*(1), 10–19, doi:10.1029/2002WR001370.

Saiers, J. E., G. M. Hornberger, D. B. Gower, and J. S. Herman (2003), The role of moving air-water interfaces in colloid mobilization within the vadose zone, *Geophys. Res. Lett.*, *30*(21), doi:10.1029/2003GL018418.

Schäfer, A., P. Ustohal, H. Harms, F. Stauffer, T. Dracos, and A. J. B. Zehnder (1998), Transport of bacteria in unsaturated porous media, *J. Contam. Hydrol.*, *33*, 149–169.

Shang, J., M. Flury, G. Chen, and J. Zhuang (2008), Impact of flow rate, water content, and capillary forces on in situ colloid mobilization during infiltration in unsaturated sediments, *Water Resour. Res.*, *44*, W06411, doi:10.1029/2007WR006516.

Shang, J., M. Flury, and Y. Deng (2009), Force measurements between particles and the air-water interface: Implications for particle mobilization in unsaturated porous media, *Water Resour. Res.*, *45*, W06420, doi:10.1029/2008WR007384.

Sharma, P., M. Flury, and J. Zhou (2008), Detachment of colloids from a solid surface by a moving air-water interface, *J. Colloid Interface Sci.*, *326*, 143–150.

Šimůnek, J., C. He, L. Pang, and S. A. Bradford (2006), Colloid-facilitated solute transport in variably saturated porous media: Numerical model and experimental verification, *Vadose Zone J.*, *5*, 1035–1047.

Sirivithayapakorn, S., and A. Keller (2003), Transport of colloids in unsaturated porous media: A pore-scale observation of processes during the dissolution of air-water interface, *Water Resour. Res.*, *39*(12), 1346, doi:10.1029/2003WR002487.

Torkzaban, S., S. M. Hassanizadeh, J. F. Schijven, A. M. de Bruin, and A. M. de Roda Husman (2006a), Virus transport in saturated and unsaturated sand columns, *Vadose Zone J.*, *5*, 877–885.

Torkzaban, S., S. M. Hassanizadeh, J. F. Schijven, and H. H. J. L. van den Berg (2006b), Role of air-water interfaces on retention of viruses under unsaturated conditions, *Water Resour. Res.*, *42*, W12S14, doi:10.1029/2006WR004904.

van Genuchten, M. (1980), A closed-form equation for predicting the hydraulic conductivity of unsaturated soils, *Soil Sci. Soc. Am. J.*, *44*, 892–898.

Veerapaneni, S., J. Wan, and T. K. Tokunaga (2000), Motion of particles in film flow, *Environ. Sci. Technol.*, *34*, 2465–2471.

Wan, J., and T. K. Tokunaga (2002), Partitioning of clay colloids at air water interfaces, *J. Colloid Interface Sci.*, *247*, 54–61, doi:10.1006/jcis.2001.8132.

Wan, J., and J. L. Wilson (1994a), Visualization of the role of the gas-water interface on the fate and transport of colloids in porous media, *Water Resour. Res.*, *30*, 11–23, doi:10.1029/93WR02403.

Wan, J., and J. L. Wilson (1994b), Colloid transport in unsaturated porous media, *Water Resour. Res.*, *30*, 857–864, doi:10.1029/93WR03017.

Wan, J. M., and T. K. Tokunaga (1997), Film straining of colloids in unsaturated porous media: Conceptual model and experimental testing, *Environ. Sci. Technol.*, *31*, 2413–2420.

Zevi, Y., A. Dathe, J. F. McCarthy, B. K. Richards, and T. S. Steenhuis (2005), Distribution of colloid particles onto interfaces in partially saturated sand, *Environ. Sci. Technol.*, *39*(18), 7055–7064, doi:10.1021/es048595b.

Zevi, Y., A. Dathe, B. Gao, B. K. Richards, and T. S. Steenhuis (2006), Quantifying colloid retention in partially saturated porous media, *Water Resour. Res.*, *42*, W12S03, doi:10.1029/2006WR004929.

Zevi, Y., A. Dathe, B. Gao, W. Zhang, B. K. Richards, and T. S. Steenhuis (2009), Transport and retention of colloidal particles in partially saturated porous media: Effect of ionic strength, *Water Resour. Res.*, *45*, W12403, doi:10.1029/2008WR007322.

Zevi, Y., J. Yan, E. Rodriguez, M. Provanovic, and S. Bryant (2010), Micromodel investigation of model pathogen transport during two-phase flow, paper presented at 2010 Land Grant and Sea Grant National Water Conference, N. C., 23 Feb.

Zhang, Q. L., S. M. Hassanizadeh, A. Raoof, M. Th. van Genuchten, and S. M. Roels (2012), Modeling virus transport and remobilization during partially saturated flow, *Vadose Zone J.*, *11*, doi:10.2136/vzj2011.0090.

Zhang, Q. L., N. K. Karadimitriou, S. M. Hassanizadeh, P. J. Kleingeld, and A. Imhof (2013), Study of colloids transport during two-phase flow using a novel polydimethylsiloxane micro-model, *J. Colloid Interface Sci.*, *141–147*, doi:10.1016/j.jcis.2013.02.041.

Zhuang, J., J. F. McCarthy, J. S. Tyner, E. Perfect, and M. Flury (2007), In situ colloid mobilization in Hanford sediments under unsaturated transient flow conditions: Effect of irrigation pattern, *Environ. Sci. Technol.*, *41*, 3199–3204, doi:10.1021/es062757h.

Zhuang, J., J. S. Tyner, and E. Perfect (2009), Colloid transport and remobilization in porous media during infiltration and drainage, *J. Hydrol.*, *377*, 112–119.

Zhuang, J., N. Goeppert, C. Tu, J. McCarthy, E. Perfect, and L. McKay (2010), Colloid transport with wetting fronts: Interactive effects of solution surface tension and ionic strength, *Water Res.*, *44*, 1270–1278, doi:10.1016/j.watres.2009.12.012.